Doxycycline Influences Microcirculation Patterns in B16 Melanoma

Baocun Sun,*,†,[1] Shiwu Zhang,*,[1,2] Danfang Zhang,* Xiaojin Yin,‡ Sen Wang,‡ Yanjun Gu,* and Yalei Wang*

*Department of Pathology, Tianjin Cancer Hospital, Tianjin Medical University, Tianjin 300060, China; †Department of Pathology, Tianjin Medical University, Tianjin 300070, China; and ‡Jiangsu Simcere Pharmaceutical Co. Ltd., Nanjing 210000, China

To examine the effects of doxycycline on invasion-related protein expression and proliferation of melanoma cells and to evaluate its effect on microcirculation patterns in melanoma, we injected murine melanoma B16 cell suspensions into the groin areas of C57BL/6 mice that were randomly divided into treatment and control groups. Eight days after tumor cell injection, we administered doxycycline intraperitoneally (ip) at a dose of 0.15 mg/g/day in the treatment group and administered a physiological saline solution to the control group. Animals were sacrificed on Day 22, and we removed and weighed tumor masses and counted the numbers of vasculogenic mimicry (VM) and endothelium-dependent vessels. Immunohistochemical staining was used to analyze the expression of matrix metalloproteinase-2 (MMP-2), matrix metalloproteinase-9 (MMP-9), vascular endothelial growth factor (VEGF), and proliferating cell nuclear antigen (PCNA). We prepared protein extracts of the tumors, and we examined the activity of MMP-2 and MMP-9 in different groups by gelatin zymography. Real-time polymerase chain reaction (PCR) was used to detect MMP-2 and MMP-9 mRNA level in the fresh tumor tissue. Doxycycline treatment partly suppressed the growth of engrafted B16 melanoma, with an inhibition rate of 35.63%. There were more VM and endothelium-dependent vessels in the control group than in the treatment group. The expression level of MMP-2 and MMP-9 in the treatment group was lower than that in the control group ($P < 0.01$, $P < 0.05$). Compared with the control group, VEGF expression was increased with doxycycline treatment. The enzyme activities of MMP-9, active-MMP-2, and MMP-2/pro-MMP-2 in the treatment group were lower than those in the control group ($P < 0.01$). MMP-2 and MMP-9 mRNA levels in the treatment group were also lower than those in the control group were. Doxycycline inhibits the growth of engrafted melanoma and results in reduced expression of MMP-2, MMP-9, and VM formations. Exp Biol Med 232:1300–1307, 2007

Key words: melanoma; doxycycline; vasculogenic mimicry; matrix metalloproteinases; endothelium-dependent vessels; angiogenesis

Introduction

Angiogenesis plays an essential role in tumor growth, and blood supply is critical for the delivery of adequate oxygen and nutrients to tumor cells. Moreover, tumor invasion and metastasis are angiogenesis dependent. In 1999, Maniotis *et al*. reported a new tumor microcirculation pattern, vasculogenic mimicry (VM), in melanoma where tumor cells mimic endothelial cells and form channels to carry the blood supply to the tumor (1, 2). VM is associated with a poor prognosis for cancer patients because the 5-year survival rate of the patients with VM is nearly zero (3, 4). There are three important elements in VM formation: the plasticity of malignant tumor cells, remodeling of the extracellular matrix (ECM), and the connection of the VM channels to the host microcirculation system (5, 6).

The expression and secretion of matrix metalloproteinases (MMPs) play an important role in ECM remodeling. MMPs are Zn^{2+}-dependent endopeptidases. MMP-2 and MMP-9 are members of the MMP family, and they can functionally degrade collagen IV in ECM, a step essential for tumor invasion and metastasis (7). Moreover, MMP-9 generates growth-proliferating signals and regulates tumor cell proliferation (8). Pharmaceutical inhibitors of MMP include members of the tetracycline family of antibiotics. Doxycycline, a member of the tetracycline family, not only inhibits MMP synthesis but also chelates Zn^{2+} (required by MMPs) and thus suppresses the activity of MMP-2 and MMP-9 (9, 10). However, doxycycline, belonging to chemically modified tetracyclines (CMTs), has proven

This work was partially supported by the National Science Foundation of China (30370554) and the Foundation of Jiangsu Simcere Pharmaceutical (Endo-005).

[1] These authors contributed equally to this work.

[2] To whom correspondence should be addressed at Department of Pathology, Tianjin Cancer Hospital, Tianjin Medical University, Tianjin 300060, PR China. E-mail: zhangshiwu666@yahoo.com.cn

Received May 25, 2007.
Accepted July 11, 2007.

DOI: 10.3181/0705-RM-145
1535-3702/07/23210-1300$15.00

disappointing as an antibiotic because of its clinical side effects (e.g., nausea, vomiting, and poor appetite). Nevertheless, its use as an anticancer agent has not been fully explored. In this study, we report the effects of doxycycline on the growth and microcirculation patterns of melanoma and on VM channel formation. Our results suggest that doxycycline may have potential as an additional tool in the treatment of solid tumors.

Material and Methods

Cells and Animals. Frozen mouse melanoma B16/F10 tissue was kindly provided by the Biochemical Department of Tianjin Cancer Hospital and Institute (Tianjin, China). Forty-seven female, 6-week old, 18–22 g C57/BL mice were purchased from Animal Center Academy of Military Medical Science (License: SCXK [Jin] 2004–0001; Beijing, China). They arrived at the Animal Centre of Tianjin Cancer Hospital 1 week before the experiment and were bred under specific pathogen-free (SPF) conditions.

Drugs and Reagent. Doxycycline-HCL powder (purity 99.99%) was purchased from Sigma Chemical Co. (St. Louis, MO) and stored at 4°C. Doxycycline powder was dissolved in sterile 0.9% NaCl at a final concentration of 20 mg/ml.

Mouse Tumor Model and Doxycycline Administration. Frozen mouse melanoma B16/F10 tissue was incubated in 40°C water for 15 mins and made into a cell suspension (1×10^7/ml). A B16/F10 melanoma cell suspension was injected into the left groin area of the mice at 0.2 ml/mouse. Forty-seven mice were randomly divided into a treatment group (24 mice) and a control group (23 mice). Eight days after tumor cells were engrafted, tumor masses were detected, and doxycycline solution was administered intraperitoneally (ip; 0.15 ml/mouse/day) in the treatment group. Mice in the control group received an equivalent 0.9% NaCl solution as a placebo. Mice were sacrificed by cervical decapitation following 14 days of continuous treatment, and the tumor masses were removed and weighed. A part of the tumor without necrosis was collected and stored at –80°C, and the remainder of each tumor was fixed with formalin and embedded in paraffin.

Tumor Growth Analysis. The length and width of each tumor were measured with a vernier caliper each day from Day 8 to Day 22 after inoculation. Tumor size was determined using the following formula: [volume (mm^3) = (length $\times$ width^2)/2]. The inhibition rate (IR) of the engrafted tumor was determined using the following formula:

$$\mathrm{IR}(\%) = \left(1 - \frac{\text{tumor weight of treatment group}}{\text{tumor weight of control group}}\right) \times 100\% \quad (1)$$

Immunohistochemical Staining and Quantification. Polyclonal antibodies used in this study were rabbit anti-MMP-2 (Boster, Wuhan, China; dilution 1:200), rabbit anti-MMP-9 (Boster; dilution 1:200), rabbit antiproliferating cell nuclear antigen (PCNA; Boster; dilution 1:100), and rabbit antivascular endothelial growth factor (VEGF; Boster; dilution 1:100). Four-micrometer sections from formalin-fixed, paraffin-embedded tissue were mounted on poly-L-lysine–coated slides. The slides were air-dried and the tissue deparaffinized. Endogenous peroxidase activity was blocked with 3% hydrogen peroxide in 50% methanol for 10 mins at room temperature. The sections were rehydrated and washed with phosphate-buffered saline (PBS) and then pretreated with citrate buffer (0.01 *M* citric acid, pH 6.0) for 20 mins at 100°C in a microwave oven. After nonspecific binding sites were blocked by incubation in 2% normal goat serum in PBS for 15 mins at 37°C. The sections were incubated overnight at 4°C with the primary antibody as indicated. The sections were then washed with PBS and incubated with the second antibody for 30 mins at 37°C. The sections were incubated with horseradish peroxidase (HRP)–conjugated antibody for 30 min at 37°C after the PBS washes. Staining was performed by incubating with fresh diaminobenzidine (DAB) buffer. The sections were washed in running water and counterstained with hematoxylin, followed by dehydration and coverslip mounting. PBS was used in place of the first antibodies as the negative control.

The sections were viewed at ×400, and 10 fields were chosen randomly. Positive cell numbers were counted in 100 random melanoma cells in every field, and the average number was used to determine the expression of the proteins in a section.

Immunohistochemical and Periodic Acid-Schiff (PAS) Histochemical Double-Staining Methods. Antibodies used in this study were mouse monoclonal anti-CD34 (Sigma Chemical), which was used at a 1:400 dilution. After CD34 immunohistochemical staining, the sections were then washed with running water for 5 mins and incubated with PAS for 15 mins. Finally, all of the sections were counterstained with hematoxylin, dehydrated, and mounted with a coverslip. Normal human stomach mucous membrane was the positive control.

VM and Endothelium-Dependent Vessel Quantification. The sections stained with PAS were viewed at ×400, and 10 fields were chosen randomly. The vessels lined by endothelial cells, regardless of the presence of basement membrane, were counted as endothelium-dependent vessels. The channels defined as VM were enclosed by melanoma cells and lined by PAS-positive material with red cells in the center of the channels. The average number of VM channel and endothelium-dependent vessels was determined.

Gelatin Zymography. When the mice were sacrificed, melanoma tissues were harvested, and the stroma was eliminated. The melanoma tissues were stored at –80°C.

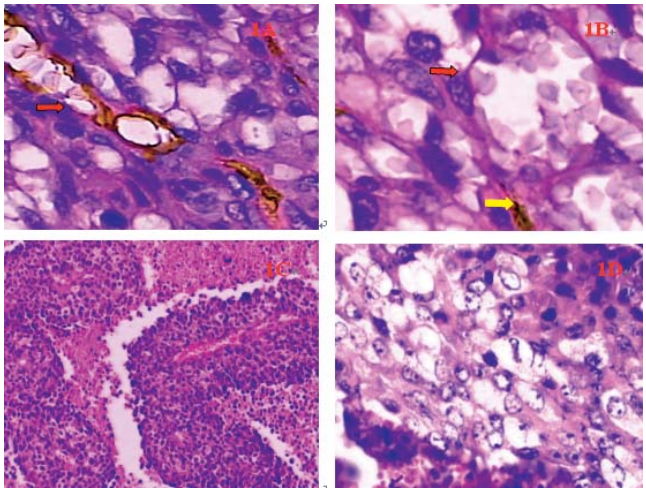

Figure 1. (A; upper left panel) Endothelium-dependent vessels (red arrow) are lined by spindle-figure endothelial cells, and the basement membrane of the vessels is positive for PAS staining. Magnification: ×400. (B; upper right panel) VM channel (red arrow) is formed by tumor cells, and there are red cells in the center of the channels. Note the absence of necrosis and hemorrhage in the tumor tissue near the VM channel. PAS-positive substances line the channel and form a basement membrane–like structure. Endothelium-dependent vessels (yellow arrow) are also present with VM, CD34, and PAS double-staining. Magnification: ×1000. (C; lower left panel) Tumor in the doxycycline-treatment group. There are several melanoma cells islands separated by necrosis in the tumor. Hematoxylin and eosin. Magnification: ×100. (D; lower right panel) Tumor cells in the treatment group. Note the vacuoles within the cytoplasm and the nuclei in the tumor cells, a feature of cell degeneration. Hematoxylin and eosin. Magnification: ×400. A color version of the figure is available in the online version of the journal.

The frozen melanoma tissues were lysed with 10% sodium dodecyl sulfate (SDS) in liquid nitrogen, and the lysates were collected and centrifuged for 10 mins at 4°C and 16,000 *g* to obtain soluble cell extract. Zymography was performed as described by Mira *et al*. (11). SDS-polyacrylamide gel electrophoresis (PAGE) was performed in a Tris-glycine buffer system with a 3% stacking gel and 12.5% separation gel. After electrophoresis, gels were incubated in 2.5% Triton X-100 for 1 hr and then digested in 50 m*M* $CaCl_2$ and 50 μ*M* $ZnCl_2$ for 48 hrs. The gels were stained with 0.1% Coomassie brilliant blue G250, and the location of proteolytic activity was detected as clear bands in a background of uniform staining. Gels were documented and analyzed using a graph analysis system. The area and gray scale of a band were measured, and the decomposed quantity of a band was counted using the following formula: band decomposed quantity = band area × (band gray scale − background gray scale) to indicate the activity of the MMPs.

Real-Time Polymerase Chain Reaction (PCR). Total RNA was extracted with Trizol reagent according to the manufacturer's instructions. cDNA was synthesized and amplified from total RNA using the Access Reverse transcriptase (RT)-PCR system (TaKaRa Bio, Inc., Otsu, Japan). The primer sequences used for MMP-2 detection were 5′-GATAACCTGGATGCCGTCGTG-3′ (sense) and 5′-CTTCACGCTCTTGAGACTTTGGTTC-3′ (antisense) with a melting temperature (Tm) for MMP-2 of 54°C, and a Tm for β-actin of 58.9°C for 35 cycles. The primer sequences used for MMP-9 detection were 5′-GCCCTGGAACTCACACGACA-3′ (sense) and 5′-TTGG-AAACTCACACGCCAGAAG-3′ (antisense) with a Tm of 53.1°C. The resultant cDNA products of MMP-2, MMP-9, and β-actin were 109, 86, and 174 bp, respectively. Real-time PCR products were analyzed with the GeneAMP PCR System 5700 Sequence Detector (Applied Biosystems, Foster City, CA), and the cycle threshold (Ct) values were evaluated.

Statistical Analysis. The data in this study were analyzed with SPSS 11.5 for Windows (SPSS Inc., Chicago, IL), and statistical significance was defined as <0.05. A *t* test was performed to compare the differences between mRNA level, protein expression, and protein activity in the two groups.

Results

Morphology of the Engrafted Melanoma. Eight days after melanoma cell injection, engrafted tumors were palpated on the mouse groin areas and detected tumors were removed. Soft globular tumors were observed, and there were numerous network vessels on the tumor surfaces. Characteristically, the nuclei were extremely dark upon staining, and the nuclear to cytoplasmic ratio approached 1:1 with numerous mitoses distributed in the tumor tissue. Some melanoma cells invaded into the skeletal muscle and showed a spindle configuration. Endothelium-dependent vessels and VM channels were observed in the tumors. CD34 and PAS double-staining revealed that there were networks formed by PAS-positive substances in the tumors, and the basement membrane of the endothelium-dependent vessels was positive for PAS (Fig. 1A). Tumor cells formed in the VM channels that were lined by PAS-positive and basement membrane–like substances, and there were red cells in the center of these channels (Fig. 1B). Moreover, no necrosis or hemorrhage in the tumor tissue near the VM channels was noted. Necrosis and hemorrhage occurred in the treatment and control groups, but the area of necrosis in the treatment group was larger than that observed in the control group (Fig. 1C). There were many melanoma islands separated by necrotic tissue in the doxycycline treatment group, and some tumor cells exhibited degeneration characteristics, with vacuoles within both cytoplasm and nuclei (Fig. 1D).

The Effect of Doxycycline on Tumor Growth. The engrafted melanomas in the doxycycline treatment group grew slower than those in the control group (Fig. 2). Fourteen days after doxycycline administration, the average size of the tumors in the treatment group was 6.212 cm^3, whereas, in the control group, the average size was 8.764 cm^3. Results from weighing the tumor masses indicated that the IR of doxycycline was 35.63%.

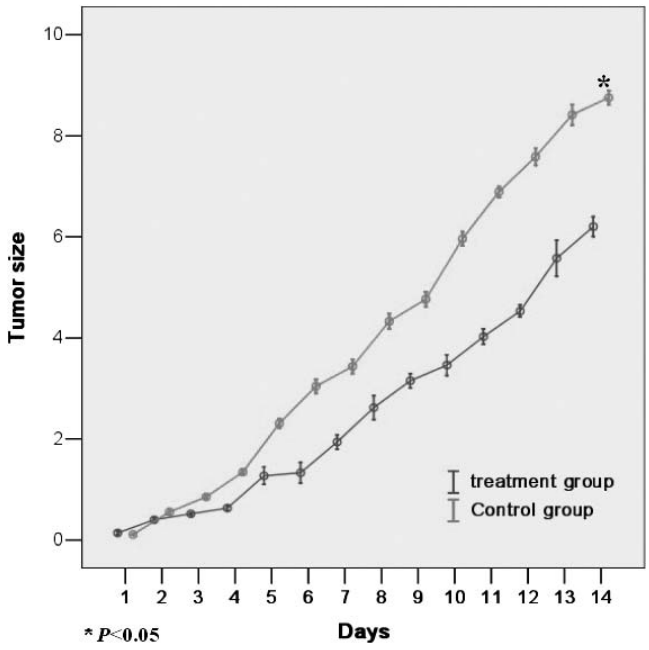

Figure 2. Tumor growth curve in the treatment and control groups. Tumor size was measured as described in the Materials and Methods.

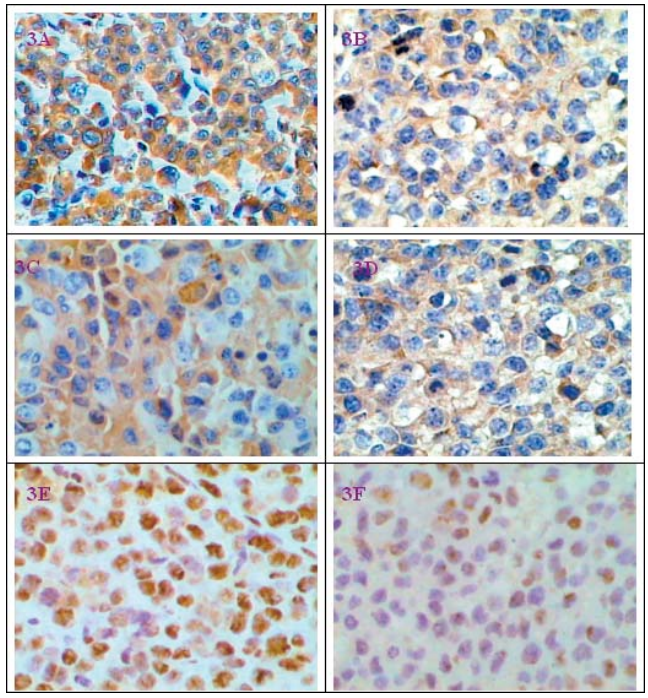

Figure 3. (A) MMP-2 expression in the control group. All of the melanoma cells are positive for MMP-2 as detected by immunohistochemical staining, and the cytoplasm of positive cells is dark brown. Immunohistochemistry (IHC). Magnification: ×400. (B) MMP-2 expression in the doxycycline-treatment group. Some melanoma cells express MMP-2, and the intensity is weak compared with the control group. IHC. Magnification: ×400. (C) MMP-9 expression in the control group. Numerous melanoma cells express MMP-9, and the cytoplasm of positive cells is dark brown. IHC. Magnification: ×400. (D) MMP-9 expression in the treatment group. Some melanoma cells express MMP-9, and the intensity is weak compared with the control group. IHC. Magnification: ×400. (E) PCNA expression in the control group. Positive melanoma cells with a diffuse brown nucleus. IHC. Magnification: ×100. (F) PCNA expression in the doxycycline-treatment group. Some melanoma cells express PCNA, and the intensity is weak compared with the control group. IHC. Magnification: ×100. A color version of the figure is available in the online version of the journal.

Analysis of VM Channel Formation. Counting the microcirculation patterns in the tumors indicated that there were fewer VM channels and endothelium-dependent vessels in the treatment group than the control group (Table 1). The treated group had 1.42 ± 0.55 endothelium-dependent vessels and 1.46 ± 0.6 VM channels compared with 2.80 ± 1.01 endothelium-dependent vessels and 2.00 ± 0.67 VM channels in the control group ($P < 0.05$).

The Influence of Doxycycline on MMP-2 and MMP-9 Expression. Both treated and control groups contained MMP-2–positive and MMP-9–positive tumor cells, and the cytoplasm was positive for MMP-2 and MMP-9 staining in both groups (Fig. 3A–D). Interestingly, the tumor cells adjacent to host tissue showed a high expression of MMP-2 and MMP-9. As shown in Table 2, tumors in the treatment group expressed less MMP-2 and MMP-9 protein than the control group ($P < 0.05$).

The Effects of Doxycycline on VEGF and PCNA Expression. Some tumor cells in both groups were positive for VEGF as determined by immunohistochemical staining. Compared with the control group, VEGF expression was upregulated in tumors obtained from the doxycycline-treated group (Table 2). PCNA was also expressed in the nuclei of both tumor groups, and at higher tumor-cell densities, more PCNA-positive cells were observed. As shown in Figure 3E and F and Table 2, the number of tumor cells positive for PCNA staining in the treatment group was less than that observed in the control group. This indicates that the tumor cells in the treatment group had a lower proliferating rate than those in the control group.

Table 1. Comparison of Endothelium-Dependent Vessels and VM Channels in the Treatment and Control Groups

Group	*n*	Endothelium-dependent vessels[a]	*P*	VM[a]	*P*
Treatment group	24	1.42 ± 0.55	$P < 0.05$	1.46 ± 0.60	$P < 0.05$
Control group	23	2.80 ± 1.01		2.00 ± 0.67	

[a] $\bar{x}$ ± SD.

Table 2. Comparison of the Expression of MMP-2, MMP-9, VEGF, and PCNA in Tumor Cells of the Treatment and Control Groups[a]

Group	*n*	MMP-2	MMP-9	VEGF	PCNA
Treatment group	24	0.330 ± 0.086	0.345 ± 0.086	0.425 ± 0.075	0.322 ± 0.106
Control group	23	0.569 ± 0.868*	0.634 ± 0.080*	0.337 ± 0.120*	0.538 ± 0.094*

[a] $\bar{x} \pm$ SD.
* $P < 0.05$.

Analysis of MMP-2 and MMP-9 Activity. The results of gelatin zymography revealed that there were three clear bands in the SDS-PAGE gel in extracts obtained from both groups of tumors (Fig. 4). These bands were identified as the 92-kDa MMP-9, 72-kDa Pro-MMP-2, and 62-kDa activated MMP-2. A 34-kDa MT1-MMP band was blurry and difficult to quantify. Statistical analysis indicated that the activities of MMP-9 and activated MMP-2 in the treatment group melanoma were less than that in the control group ($P < 0.01$), but as shown in Table 3, there was no significant difference in the activity of Pro-MMP-2.

Results of Real-Time RT-PCR. Real-time PCR demonstrated that the expression of MMP-2 and MMP-9 mRNA in the experiment group was decreased compared with the control group. The Ct values of MMP-2 and MMP-9 in the control and experiment groups are listed in Table 4. The difference between MMP-2 and MMP-9 Ct values was statistically significant ($P < 0.01$). The results suggested that doxycycline could inhibit tumor growth *via* down-regulating the MMP-2 mRNA level.

Discussion

It had been believed that endothelium-dependent vessels were the only microcirculation mechanism present in tumors, so endothelial cells have been the target of traditional antiangiogenesis treatment for solid tumors (12, 13). However, VM, an endothelium-independent microcirculation pattern, has been demonstrated to exist in many malignant tumor types. This finding suggests that the VM channel should be an additional target in an antiangiogenesis strategy to treat solid tumors (14, 15). In this study, B16 melanoma tumor cell growth was reduced by doxycycline treatment. Fourteen days after doxycycline administration, IR for engrafted melanoma was 35.63%. In support of this reduction of tumor size, we observed that the doxycycline treatment group had less endothelium-dependent vessels and fewer VM channels than those in the control group, and the expression and activity of MMP-2 and MMP-9 were lower in the treatment group than in the control group. These findings indicate that doxycycline inhibited melanoma angiogenesis through inhibition/reduction of MMP activity. Furthermore, compared with the tumors in the control group, large areas of necrosis were observed in tumors in the treatment group. These results support the hypothesis that the blood supply from endothelium-dependent vessels and VM channels was blocked by doxycycline administration, leading to necrosis and tumor reduction.

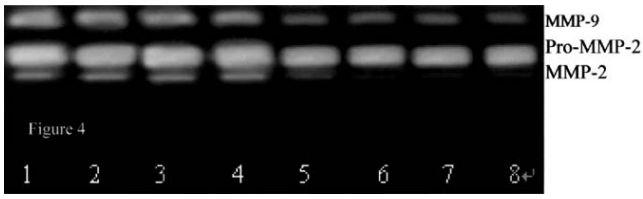

Figure 4. Gelatin zymography. Lanes 1–4, control group. Lanes 5–8, the doxycycline-treatment group. The 92-kDa MMP-9, 72-kDa Pro-MMP-2, and 62-kDa activated-MMP-2 are observed in both groups. The 34-kDa MT1-MMP is blurry and was not analyzed. Enzyme levels were determined as described in the Materials and Methods.

Tetracycline is an efficient antibiotic drug, but it has dose-dependent side effects (16, 17). In this study, mice treated with doxycycline *via* IP had no obvious side effects, demonstrating that these antibiotics may be useful as anticancer agents at doses that exhibit fewer side effects. Tetracycline can inhibit the activity and function of MMPs (18), and doxycycline, a member of the tetracycline family, has a potent effect on the synthesizing and activity of MMPs (19–21). However, the molecular mechanism involved in these effects of doxycycline is still not clear. There are several possible explanations that should be considered: (i) doxycycline may reduce the stability of MMP mRNA (22–24); (ii) doxycycline chelates Zn^{2+}, which is required for MMP activity; (iii) doxycycline may eliminate reactive oxygen species (ROS) secreted by extracellular matrix cells and thus block the activation of pro-MMPs; and (iv) doxycycline may inhibit the activation of MMPs *via* the MT1-MMP pathway (25–28). The precise mechanism by which doxycycline functions awaits further experimentation.

MMP-2 and MMP-9 are both members of the MMP family that are secreted as inactivated zymogens (72 kDa and 92 kDa, respectively) and need to be activated by proteolytic cleavage into active forms (62 kDa and 88 kDa, respectively; Refs. 29, 30). The result of anti-MMP-2 and MMP-9 immunohistochemical staining revealed that the expression of these proteins in tumors from the doxycycline-treated group was less than that observed in the control group. This may be associated with a reduction of MMP mRNA stability (31, 32). Moreover, there was no significant difference in pro-MMP-2 levels between the 2 groups, whereas the activity of MMP-2 and MMP-9 in the treatment

Table 3. Comparison of the Activity of MMP-9, Pro-MMP-2, and MMP-2 in the Melanoma of the Treatment and Control Groups[a]

Group	*n*	MMP-9	Pro-MMP-2	MMP-2	MMP-2 to pro-MMP-2 ratio
Treatment group	24	24.99 ± 2.30	121.35 ± 8.53	7.40 ± 1.82	6.10%
Control group	23	46.18 ± 4.65*	126.07 ± 4.73**	25.93 ± 3.30*	20.65%

[a] $\bar{x} \pm$ SD.
* $P < 0.01$; ** $P < 0.05$.

group decreased as compared with the control group. This suggests that doxycycline inhibited the activated MMP-2 and MMP-9 thus inhibiting tumor growth and angiogenesis.

Endothelium-dependent vessels and VM channels both contribute to the microcirculation patterns in the B16 melanoma model described in this report. The presence of both microcirculation systems not only meet the need for oxygen and nutrients required for tumor growth but also enhance metastasis (33). MMP family members, especially MMP-2 and MMP-9, play important roles in endothelium-dependent vessels and VM channel formation (34). MMPs activate the angiogenesis switch, decompose ECM, and provide the space for vessel formation. It is important for endothelial cells to migrate through ECM and the fiber network during endothelium-dependent vessels formation. Collagen IV is a major constituent of basement membrane ECM, and a major function of MMP-2 and MMP-9 is to degrade collagen IV, resulting in promotion of angiogenesis (34, 35). Furthermore, MMP-9 can induce VEGF secretion into the ECM, resulting in enhanced tumor angiogenesis (36).

Microarray analyses revealed that MMPs-1, –2, –9, and MT1-MMP are all more highly expressed in aggressive melanoma with VM channels compared with poorly aggressive melanomas that lack VM channels (37). Phosphoinositide-3 kinase (PI3K) is a key signal in VM channel formation when pro-MMP-2 is activated, converted into active MMP-2, which then cleaves laminin (38). Laminins are major constituents of basement membrane ECM and are thought to stabilize the organization of the basement membrane. The degradation of laminin contributes to the integrin-mediated migratory behavior of melanoma cells. Seftor *et al.* (35) suggested that the fragments of activated MMP-2 from highly aggressive melanoma cells induced VM channel formation in poorly aggressive melanoma. Hence, inhibitors of MMP may have a negative effect on melanoma invasion and metastases by inhibiting VM formation. Seftor *et al.* (39) observed that doxycycline reduced the lung metastases of human melanoma C8161 in severe combined immunodeficiency disorder (SCID) mice. They suggested that doxycycline exerts a negative influence on melanoma aggression and metastases through multiple mechanisms. Thus, inhibition of MMPs represents an important molecular target in the treatment of solid tumors.

Table 4. Comparison of MMP-2 and MMP-9 mRNA in Melanoma Between the Treatment and Control Groups[a]

Group	*n*	MMP-2	MMP-9
Treatment group	24	23.80 ± 0.98	24.16 ± 0.79
Control group	23	18.43 ± 0.47*	20.28 ± 0.81*

[a] $\bar{x} \pm$ SD.
* $P < 0.01$.

In addition to the role of MMPs in the angiogenesis process, VEGF is considered one of the most important factors promoting angiogenesis. Many normal and tumor cells can synthesize and secrete VEGF, resulting in paracrine effects on the behavior and function of endothelial cells (40). The interaction of VEGF with its receptor (flt-1 or KDR/flt-1) on the surface of endothelial cells leads to the migration and proliferation of those cells. The expression of VEGF is regulated indirectly by oxygen concentration and hypoxia, conditions that enhance the expression and stability of VEGF mRNA (41). Rapid growth of tumors results in the hypoxic conditions that stimulate VEGF expression and promote tumor angiogenesis. In our study, we observed that VEGF expression in the tumors increased in the doxycycline-treated animals, whereas VM channel and endothelium-dependent vessels were reduced as compared with the control group. These data suggest that microcirculation patterns were inhibited by doxycycline administration, aggravating hypoxia, and increasing VEGF expression.

Recently, it has been reported that doxycycline affects the cell cycle and inhibits tumor cell proliferation (42). Doxycycline blocks protein synthesis, reduces the supply of ATP, and disturbs the energy metabolism of the tumor cell, inhibiting tumor cell growth (43). PCNA is a protein involved in mediating DNA replication, and the results from our study demonstrated that the expression of PCNA decreased after 14 days of doxycycline treatment. Thus, our data are consistent with a model where doxycycline also has a role in decreasing tumor cell proliferation.

In summary, in this report, we demonstrate that the effects of doxycycline on the microcirculation patterns in the B16 mouse melanoma involve inhibition of microcirculation formation and activity of matrix metalloproteinases. The dose of 0.15 mg/g/day for IP in mouse is equal to about 180 mg/day for an adult with oral administration. It is

reported doxycycline at a dose of 200 mg/day/person exhibits few side-effects, other than some discomfort of the digestive tract (44). In this study, mice in the treatment group showed neither poor appetite nor loss of weight. Moreover, compared with the benefit of the anticancer effect, the side effects are negligible. These data provide a basis for considering tetracycline-based antibiotics for use in antiangiogenesis treatment of solid tumors.

We thank Dr. Howard for his editorial assistance.

1. Maniotis AJ, Folberg R, Hess A, Seftor EA, Gardner LM, Pe'er J, Trent JM, Meltzer PS, Hendrix MJ. Vascular channel formation by human melanoma cells in vivo and in vitro: vasculogenic mimicry. Am J Pathol 155:739–752, 1999.
2. Slipicevic A, Holm R, Nguyen MT, Bohler PJ, Davidson B, Florenes VA. Expression of activated Akt and PTEN in malignant melanomas: relationship with clinical outcome. Am J Clin Pathol 124:528–536, 2005.
3. Sun B, Zhang S, Zhao X, Zhang W, Hao X. Vasculogenic mimicry is associated with poor survival in patients with mesothelial sarcomas and alveolar rhabdomyosarcomas. Int J Oncol 25:1609–1614, 2004.
4. Sun B, Zhang S, Ni C, Zhang D, Zhao X. The clinical significance study of vasculogenic mimicry in 337 cases of bi-directional differential malignant tumors. Chin J Clin Oncol 32:64–67, 2005.
5. Folberg R, Hendrix MJ, Maniotis AJ. Vasculogenic mimicry and tumor angiogenesis. Am J Pathol 156:361–381, 2000.
6. Zhang S, Guo H, Zhang D, Zhang W, Zhao X, Ren Z, Sun B. Microcirculation patterns in different stages of melanoma growth. Oncol Rep 15(1):15–20, 2006.
7. Curran S, Murray GI. Matrix metalloproteinases: molecular aspects of their roles in tumour invasion and metastasis. Eur J Cancer 36:1621–1630, 2000.
8. Ishizaki T, Katsumata K, Tsuchida A, Wada T, Mori Y, Hisada M, Kawakita H, Aoki T. Etodolac, a selective cyclooxygenase-2 inhibitor, inhibits liver metastasis of colorectal cancer cells via the suppression of MMP-9 activity. Int J Mol Med 17:357–362, 2006.
9. Seftor RE, Seftor EA, Kirschmann DA, Hendrix MJ. Targeting the tumor microenvironment with chemically modified tetracyclines: inhibition of laminin 5 γ2 chain promigratory fragments and vasculogenic mimicry. Mol Cancer Ther 1:1173–1179, 2002.
10. Liu J, Xiong W, Baca-Regen L, Nagase H, Baxter BT. Mechanism of inhibition of matrix metalloproteinase-2 expression by doxycycline in human aortic smooth muscle cells. J Vasc Surg 38:1376–1383, 2003.
11. Mira E, Lacalle RA, Buesa JM, de Buitrago GG, Jimenez-Baranda S, Gomez-Mouton C, Martinez AC, Manes S. Secreted MMP9 promotes angiogenesis more efficiently than constitutive active MMP9 bound to the tumor cell surface. J Cell Sci 117:1847–1857, 2004.
12. Getmanova EV, Chen Y, Bloom L, Gokemeijer J, Shamah S, Warikoo V, Wang J, Ling V, Sun L. Antagonists to human and mouse vascular endothelial growth factor receptor 2 generated by directed protein evolution in vitro. Chem Biol 13:549–556, 2006.
13. Matsuda KM, Madoiwa S, Hasumi Y, Kanazawa T, Saga Y, Kume A, Mano H, Ozawa K, Matsuda M. A novel strategy for the tumor angiogenesis-targeted gene therapy: generation of angiostatin from endogenous plasminogen by protease gene transfer. Cancer Gene Ther 7:589–596, 2000.
14. Van der Schaft DW, Seftor RE, Seftor EA, Hess AR, Gruman LM, Kirschmann DA, Yokoyama Y, Griffioen AW, Hendrix MJ. Effects of angiogenesis inhibitors on vascular network formation by human endothelial and melanoma cells. J Natl Cancer Inst 96:1473–1477, 2004.
15. Ruf W, Seftor EA, Petrovan RJ, Weiss RM, Gruman LM, Margaryan NV, Seftor RE, Miyagi Y, Hendrix MJ. Differential role of tissue factor pathway inhibitors 1 and 2 in melanoma vasculogenic mimicry. Cancer Res 63:5381–5389, 2003.
16. Ramamurthy NS, Vernillo AT, Greenwald RA, Lee HM, Sorsa T, Golub LM, Rifkin BR. Reactive oxygen species activate and tetracyclines inhibit rat osteoblast collagenase. J Bone Miner Res 8: 1247–1253, 1993.
17. Lee HM, Golub LM, Cao J, Teronen O, Laitinen M, Salo T, Zucker S, Sorsa T. CMT-3, a non-antimicrobial tetracycline (TC), inhibits MT1-MMP activity: relevance to cancer. Curr Med Chem 8:257–260, 2001.
18. Rodriguez-Manzaneque JC, Lane TF, Ortega MA, Hynes RO, Lawler J, Iruela-Arispe ML. Thrombospondin-1 suppresses spontaneous tumor growth and inhibits activation of matrix metalloproteinase-9 and mobilization of vascular endothelial growth factor. Proc Natl Acad Sci U S A 98:12485–12490, 2001.
19. Isayeva T, Kumar S, Ponnazhagan S. Anti-angiogenic gene therapy for cancer. Int J Oncol 25:335–343, 2004.
20. Eisen D, Hakim MD. Minocycline-induced pigmentation. Incidence, prevention and management. Drug Saf 18:431–440, 1998.
21. Teitelbaum JE, Perez-Atayde AR, Cohen M, Bousvaros A, Jonas MM. Minocycline-related autoimmune hepatitis: case series and literature review. Arch Pediatr Adolesc Med 152:1132–1136, 1998.
22. Morrison CJ, Butler GS, Bigg HF, Roberts CR, Soloway PD, Overall CM. Cellular activation of MMP-2 (gelatinase A) by MT2-MMP occurs via a TIMP-2-independent pathway. J Biol Chem 276:47402–47410, 2001.
23. Bernardo MM, Fridman R. TIMP-2(tissue inhibitor of metalloproteinase-2) regulates MMP-2 (matrix metalloproteinase-2) activity in the extracellular environment after pro-MMP-2 activation by MT1 (membrane type 1)-MMP. Biochem J 374:739–745, 2003.
24. Basset P, Bellocq JP, Wolf C, Stoll I, Hutin P, Limacher JM, Podhajcer OL, Chenard MP, Rio MC, Chambon P. A novel metalloproteinase gene specifically expressed in stromal cells of breast carcinomas. Nature 348:699–704, 1990.
25. Nelson AR, Fingleton B, Rothenberg ML, Matrisian LM. Matrix metalloproteinases: biologic activity and clinical implications. J Clin Oncol 18:1135–1149, 2000.
26. Olson MW, Toth M, Gervasi DC, Sado Y, Ninomiya Y, Fridman R. High affinity binding of latent matrix metalloproteinase-9 to the α2(IV) chain of collagen IV. J Biol Chem 273:10672–10681, 1998.
27. Folkman J. Tumor angiogenesis: therapeutic implications. N Engl J Med 285:1182–1186, 1971.
28. Shirakawa K, Kobayashi H, Sobajima J, Hashimoto D, Shimizu A, Wakasugi H. Inflammatory breast cancer: vasculogenic mimicry and its hemodynamics of an inflammatory breast cancer xenograft model. Breast Cancer Res 5:136–139, 2003.
29. Shirakawa K, Kobayashi H, Heike Y, Kawamoto S, Brechbiel MW, Kasumi F, Iwanaga T, Konishi F, Terada M, Wakasugi H. Hemodynamics in vasculogenic mimicry and angiogenesis of inflammatory breast cancer xenograft. Cancer Res 62:560–566, 2002.
30. Fang J, Shing Y, Wiederschain D, Yan L, Butterfield C, Jackson G, Harper J, Tamvakopoulos G, Moses MA. Matrix metalloproteinase-2 is required for the switch to the angiogenic phenotype in a tumor model. Proc Natl Acad Sci U S A 97:3884–3889, 2000.
31. Uitto VJ, Firth JD, Nip L, Golub LM. Doxycycline and chemically modified tetracyclines inhibit gelatinase A (MMP-2) gene expression in human skin keratinocytes. Ann N Y Acad Sci 732:140–151, 1994.
32. Jonat C, Chung FZ, Baragi VM. Transcriptional downregulation of stromelysin by tetracycline. J Cell Biochem 60:341–347, 1996.
33. Folberg R, Maniotis AJ. Vasculogenic mimicry. APMIS 112:508–525, 2004.
34. Sood AK, Seftor EA, Fletcher MS, Gardner LM, Heidger PM, Buller RE, Seftor RE, Hendrix MJ. Molecular determinants of ovarian cancer plasticity. Am J Pathol 158:1279–1288, 2001.

35. Seftor RE, Seftor EA, Koshikawa N, Meltzer PS, Gardner LM, Bilban M, Stetler-Stevenson WG, Quaranta V, Hendrix MJ. Cooperative interactions of laminin 5 γ2 chain, matrix metalloproteinase-2, and membrane type-1-matrix/metalloproteinase are required for mimicry of embryonic vasculogenesis by aggressive melanoma. Cancer Res 61: 6322–6327, 2001.
36. Zaman K, Driscoll R, Hahn D, Werffeli P, Goodman SL, Bauer J, Leyvraz S, Lejeune F, Stupp R, Ruegg C. Monitoring multiple angiogenesis-related molecules in the blood of cancer patients shows a correlation between VEGF-A and MMP-9 levels before treatment and divergent changes after surgical vs. conservative therapy. Int J Cancer 118:755–764, 2006.
37. Hendrix MJ, Seftor EA, Kirschmann DA, Quaranta V, Seftor RE. Remodeling of the microenvironment by aggressive melanoma tumor cells. Ann N Y Acad Sci 995:151–161, 2003.
38. Hess AR, Seftor EA, Seftor RE, Hendrix MJ. Phosphoinositide 3-kinase regulates membrane Type 1-matrix metalloproteinase (MMP) and MMP-2 activity during melanoma cell vasculogenic mimicry. Cancer Res 63:4757–4762, 2003.
39. Seftor RE, Seftor EA, De Larco JE, Kleiner DE, Leferson J, Stetler-Stevenson WG, McNamara TF, Golub LM, Hendrix MJ. Chemically modified tetracyclines inhibit human melanoma cell invasion and metastasis. Clin Exp Metastasis 16:217–225, 1998.
40. Cleaver O, Melton DA. Endothelial signaling during development. Nat Med 9:661–668, 2003.
41. Pore N, Jiang Z, Gupta A, Cerniglia G, Kao GD, Maity A. EGFR tyrosine kinase inhibitors decrease VEGF expression by both hypoxia-inducible factor (HIF)-1-independent and HIF-1-dependent mechanisms. Cancer Res 66:3197–204, 2006.
42. Onoda T, Ono T, Dhar DK, Yamanoi A, Fujii T, Nagasue N. Doxycycline inhibits cell proliferation and invasive potential: combination therapy with cyclooxygenase-2 inhibitor in human colorectal cancer cells. J Lab Clin Med 143:207–216, 2004.
43. Suzuki A, Yagisawa J, Kumakura S, Tsutsui T. Effects of minocycline and doxycycline on cell survival and gene expression in human gingival and periodontal ligament cells. J Periodontal Res 41:124–131, 2006.
44. Sun BC, Zhang SW, Qi LS, Zhang DF, Guo H, Zhao XL. Study on the molecular mechanism of endostatin and doxycycline in suppressing melanoma growth. Zhonghua Bing Li Xue Za Zhi 35:677–680, 2006.